Appendix I

High Resolution Sub-Millimeter Spectroscopy Using
Mode-Locked Laser Driven Electro-Optic Antennas

20000628 022

DTIC QUALITY INSPECTED 4

REPORT DOCUMENTATION PAGE

Form Approved
OMB NO. 0704-0188

Public Reporting burden for this collection of information is estimated to average 1 hour per response, including the time for reviewing instructions, searching existing data sources, gathering and maintaining the data needed, and completing and reviewing the collection of information. Send comment regarding this burden estimates or any other aspect of this collection of information, including suggestions for reducing this burden, to Washington Headquarters Services, Directorate for information Operations and Reports, 1215 Jefferson Davis Highway, Suite 1204, Arlington, VA 22202-4302, and to the Office of Management and Budget, Paperwork Reduction Project (0704-0188.) Washington, DC 20503.

1. AGENCY USE ONLY (Leave Blank)	2. REPORT DATE	3. REPORT TYPE AND DATES COVERED
	16 May 2000	Final Report

4. TITLE AND SUBTITLE: Spectral purity and sources of noise in femtosecond demodulation THz sources driven by Ti:sapphire mode-locked lasers

5. FUNDING NUMBERS: DAAH04-93-D-0002

6. AUTHOR(S): Bob D. Guenther

7. PERFORMING ORGANIZATION NAME(S) AND ADDRESS(ES): Duke University Box 90305, Durham NC

8. PERFORMING ORGANIZATION REPORT NUMBER

9. SPONSORING / MONITORING AGENCY NAME(S) AND ADDRESS(ES): U. S. Army Research Office, P.O. Box 12211, Research Triangle Park, NC 27709-2211

10. SPONSORING / MONITORING AGENCY REPORT NUMBER: ARO 31412.6-PH

11. SUPPLEMENTARY NOTES

The views, opinions and/or findings contained in this report are those of the author(s) and should not be construed as an official Department of the Army position, policy or decision, unless so designated by other documentation.

12 a. DISTRIBUTION / AVAILABILITY STATEMENT	12 b. DISTRIBUTION CODE
Approved for public release; distribution unlimited.	

13. ABSTRACT (Maximum 200 words)

Direct measurements of the spectral purity in THz femtosecond demodulation sources are reported and compared to theory. Because these sources operate at very high harmonics (~102 - 104) of the mode-lock frequency, a high spectral purity source is very dependent on a low jitter femtosecond laser. Conversely, the spectral content of the THz sources provides detailed information about timing jitter and stringent tests of models used to describe the jitter. We find that both the behavior of the central core and the noise skirts of the power spectrum of our sources can be quantitatively related to measured ripple and continuum amplitude noise on the Ar+ pump laser by use of modulation theory.

14. SUBJECT TERMS	15. NUMBER OF PAGES
Demodulated Terrahertz sources, noise properties	
	16. PRICE CODE

17. SECURITY CLASSIFICATION OR REPORT	18. SECURITY CLASSIFICATION ON THIS PAGE	19. SECURITY CLASSIFICATION OF ABSTRACT	20. LIMITATION OF ABSTRACT
UNCLASSIFIED	UNCLASSIFIED	UNCLASSIFIED	UL

NSN 7540-01-280-5500

Standard Form 298 (Rev.2-89)
Prescribed by ANSI Std. 239-18
298-102

Enclosure 1

DTIC QUALITY INSPECTED 4

Forward:

A mode locked laser driven electro-optic antenna was used as a continuously tunable, high resolution, high accuracy millimeter/sub-millimeter wave spectroscopic source. To establish the limits of this source, a detailed study of the laser phase noise and its sources was undertaken.

Appendixe I: Paper entitled "High resolution sub-millimeter spectroscopy using mode-locked laser driven electro-optic antennas

Appedixe II: Spectral purity and sources of noise in femtosecond demodulation THz sources driven by Ti:sapphire mode-locked lasers.

Problem:

Develop new, tunable sources for submillimeter wave spectroscopy.

Results:

Direct measurements of the spectral purity in THz femtosecond demodulation sources are reported and compared to theory. Because these sources operate at very high harmonics (~102 - 104) of the mode-lock frequency, a high spectral purity source is very dependent on a low jitter femtosecond laser. Conversely, the spectral content of the THz sources provides detailed information about timing jitter and stringent tests of models used to describe the jitter. We find that both the behavior of the central core and the noise skirts of the power spectrum of our sources can be quantitatively related to measured ripple and continuum amplitude noise on the Ar+ pump laser by use of modulation theory.

Publications:

1. T. M. Goyette, W. Guo, F. C. De Lucia, J. Swartz, H. O. Everitt, B. D. Guenther, and E. R. Brown, "Femtosectond Demodulation Source for High Resolution Submillimeter Spectroscopy," *Appl. Phys. Lett.*, vol. 67, pp. 3810-3812, 1995.

2. "New Spectroscopic Methods for Submillimeter Plasma Diagnostic", Invited Paper, 3rd International Conference on Reactive Plasmas and 14th Symposium on Plasma Processing, January 21-24, 1997 Nara-ken New Public Hall, Nara, Japan sponsored by The Japan Society of Applied Physics cosponsored by Nagoya Industrial Research Institute.

3. Spectral purity and sources of noise in femtosecond demodulation THz sources driven by Ti:sapphire mode-locked lasers, in preparation.

Participants:

Kimberly Ann Juvan: PhD, Duke University, 1997.
John Swartz: Post doc
Kyle Ferrio: Post doc

Inventions:

NA

High Resolution Sub-Millimeter Spectroscopy Using Mode-Locked Laser Driven Electro-Optic Antennas

T.M. Goyette[1], *W. Guo*[1], *F.C. De Lucia*[1], *E.R. Brown*[2], *K.A. McIntosh*[2], *K. Juvan*[3], *J.C. Swartz*[3], *H.O. Everitt*[3,†], *and B.D. Guenther*[3,†]

[1]Ohio State Univ., Dept of Physics, Columbus, OH 43210, USA
[2]MIT Lincols Labs, Lexington, MA 02173, USA
[3]Duke Univ., Physics, Durham, NC 27708, USA

Abstract

We use a mode-locked laser driven electro-optic antenna as a continuously tunable, high resolution (<1 MHz), high absolute accuracy (1:10^7) millimeter/sub-millimeter spectroscopic source and to investigate laser phase noise.

We report the use of a mode-locked laser driven electro-optic antenna (EOA) as a continuously tunable, millimeter and sub-millimeter (MM/SMM) source for high resolution spectroscopy and laser jitter noise investigations. In this application the EOA generates MM/SMM radiation by optical down-conversion of the pulse train[1, 2]. Although previous efforts have generated MM/SMM radiation from EOAs driven by heterodyned CW lasers [3] or mode-locked lasers [4-8], these past applications have produced only low resolution (typically > 100 MHz) spectra of materials. Our work focuses on the high resolution spectroscopic capabilities of mode-locked laser driven EOA sources and their noise properties. Among their most important attributes are straightforward absolute frequency calibration and very high spectral purity.

The experimental system is shown in Fig. 1. A femtosecond mode-locked Ti:Sapphire laser of standard design drives the EOA. A translation stage on the high reflectivity mirror, M1, allows us to vary the cavity length and sweep the frequencies of the spectral components. For a laser cavity length, l, the frequency, f_m, of the mth spectral component is $f_m = cm/2l$ where c is the speed of light. A motor-driven micrometer with 1 μm step size, produces coarse frequency scanning with a resolution of $\Delta f_m = - f_m \Delta l/l$ (e.g., 187 kHz at 340 GHz). An attached piezo-electric transducer (PZT) provides even higher precision scanning or frequency modulation. The mode-locked laser drives a planar, self-complementary three turn log spiral antenna fabricated on low temperature grown GaAs [3] . The photo-current generated MM/SMM radiation from the antenna has a spectrum similar to the laser pulse train envelope limited by the EOA carrier lifetime and RC time constants. The emitted MM/SMM radiation travels off a dispersive FIR echelette grating (0.58 lines/mm), through a gas cell, and into a ^{3}He cooled bolometer. Replacing the gas cell with a Fourier transform spectrometer provides spectral diagnostics. The spectral output from the grating (Fig. 2) contains many (100-1000) components at the harmonics of the mode-lock frequency. In this experiment the low pressure (<20 mTorr) gas molecules in the cell absorb a single MM/SMM component. A lock-in amplifier tuned to twice the PZT modulation frequency measures the second derivative shape of the single absorption line. A MM/SMM hetrodyne spectrum analyzer also monitors EOA spectral components.

To demonstrate the high resolution capability of the system, we measured the absorption spectrum of OCS at 300 K. Setting the laser repetition rate to 82.413285 MHz (referenced to WWVB) places the 4131st harmonic near the J=27->28 OCS absorption frequency. Figure 3 shows the measured second derivative line shape of the OCS line whose measured line center at 340.4492 GHz is in excellent agreement with the predicted value (340.4493 GHz) and whose modulation broadened linewidth is 1.4 MHz.

These results suggest that the contribution of jitter-induced phase noise to the width of the spectral component is less than modulation broadened linewidth of the spectroscopic line. Using a quadratic scaling of phase noise with harmonic number [9], phase noise of -100 dBc at 1 kHz [10] of the 25th harmonic would scale to a linewidth of -22 dBc at 1 kHz for the 4131th harmonic . Direct measurements of the scaling of the phase noise between the 10th and 1000th harmonic are underway, and will be presented along with predictions based on various noise models [9, 11].

The results presented here demonstrate to our knowledge the first *high resolution* sub-millimeter measurement using a mode-locked laser driven electro-optic antenna. The overall system gives high absolute accuracy and resolution (~1:10^7) and provide an opportunity to

Springer Series in Chemical Physics, Volume 62
Ultrafast Phenomena X
Eds.: P.F. Barbara, J.G. Fujimoto, W.H. Knox, and W. Zinth
© Springer-Verlag Berlin Heidelberg 1996

investigate the scaling properties of noise with high harmonic number. We believe pulsed-laser-driven EOAs will find wide application in high resolution spectroscopy.

The authors would like to acknowledge the support of the NRC (JCS) and the US Army Research Office.

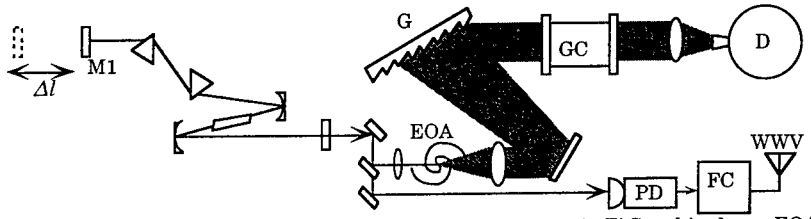

Fig. 1. Sub-millimeter-wave spectrometer: M1, moving mirror in Ti:Sapphire laser; EOA, electro-optical log spiral antenna; G, grating; GC, gas cell; D, ^{3}He bolometer; PD, photo-diode; FC, frequency counter.

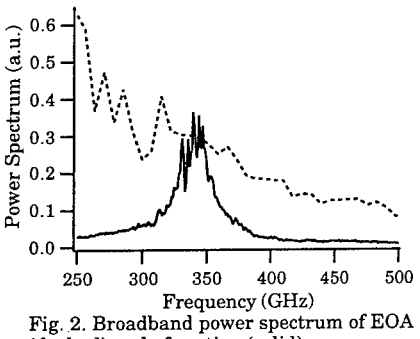

Fig. 2. Broadband power spectrum of EOA (dashed) and of grating (solid).

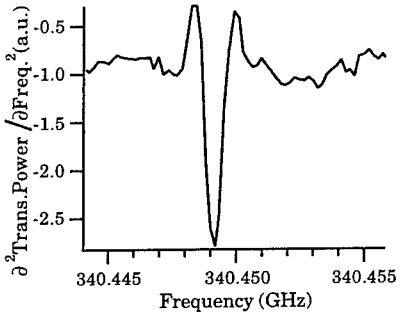

Fig. 3. Measured second derivative line shape of OCS at 340.4492 GHz.

References

1. D. H. Auston, K. P. Cheung and P. R. Smith, Appl. Phys. Lett., **45 (3)** (1984) 284-286.
2. F. C. De Lucia, B. D. Guenther and T. Anderson, Appl. Phys. Lett., **47** (1985) 894-6.
3. E. R. Brown, K. A. McIntosh, K. B. Nichols and C. L. Dennis, Appl. Phys. Lett., **66** (1995) 285.
4. D. H. Auston and M. C. Nuss, IEEE Jrn. Quant. Elect., **24** (1988) 184-197.
5. G. Arjavalingam, Y. Pastol, J.-M. Halbout and G. V. Kopcsay, IEEE MTT-**38** (1990) 615-21.
6. D. Grischkowsky, S. Keiding, M. van Exter and C. Fattinger, JOSA-B, **7** (1990) 2006-15.
7. H. Harde, N. Katzenellenbogen and D. Grischkowsky, JOSA-B, **11** (1994) 1018.
8. M. van Exter, C. Fattinger and D. Grischkowsky, Opt. Lett., **14** (1989) 1128-30.
9. D. von der Linde, Applied Physics - B, **39** (1986) 201-17.
10. J. Son, J. V. Rudd and J. F. Whitaker, Opt. Lett., **17** (1992 May 15) 733-5.
11. H. A. Haus and A. Mecozzi, IEEE Jrn. Quant. Elect., **QE-29** (1993) 983-96.

† Current address, Army Research Office, Research Triangle Park, NC 27709.

Appendix II

Spectral purity and sources of noise in femtosecond demodulation THz sources driven by Ti:sapphire mode-locked lasers.

ABSTRACT

Direct measurements of the spectral purity in THz femtosecond demodulation sources are reported and compared to theory. Because these sources operate at very high harmonics (~10^2 - 10^4) of the mode-lock frequency, a high spectral purity source is very dependent on a low jitter femtosecond laser. Conversely, the spectral content of the THz sources provides detailed information about timing jitter and stringent tests of models used to describe the jitter. We find that both the behavior of the central core and the noise skirts of the power spectrum of our sources can be quantitatively related to measured ripple and continuum amplitude noise on the Ar^+ pump laser by use of modulation theory.

I. INTRODUCTION

In an earlier letter we reported a tunable high resolution source for the mm/submm (or THz) region which is based on the demodulation of a train of femtosecond optical pulses by an electro-optical switch[1]. We have also discussed earlier work which used a synch-pumped picosecond laser system and demodulation based on a photocathode[2]. In the former, the high resolution of the femtosecond demodulation source was demonstrated by the observation of a Doppler limited spectral line of width ~ 1 MHz at 300 GHz, one of the more stringent tests of resolution for a source in this region. In contrast, the resolution of most other femtosecond laser driven THz spectroscopy sources is obtained interferometrically and is typically 0.01 cm^{-1} (300 MHz)-0.1 cm^{-1} (3000MHz)[3, 4].

In this paper we report direct measurements of the spectral purity of the femtosecond demodulation source by use of electronic spectral analysis techniques. We will compare the results obtained for the source when driven by a Ti:Sapphire laser whose mode-lock frequency is near 82 MHz[5] with those for a new system driven by a Ti:Sapphire laser whose mode-lock frequency is near 800 MHz[6-8].

Our application is closely related to the timing jitter problem, and its related power spectrum, which has been considered extensively[9-11]. Since our femtosecond demodulation THz sources operate at a high harmonic number, n_h = ~100 - 10000 and high spectral purity is important, the impact of this jitter on spectral purity at high harmonic is a significant issue. Conversely, observation of spectral content at very high harmonic is an exceptionally sensitive test of both noise theory and the laser systems themselves.

In frequency standards it is well known from classical metrology that the amplitude of the spectral skirts around the carrier (which arise from phase noise) grows as the square of the harmonic number n_h^2. Similarly, it has been shown that the amplitude of the noise in the power spectrum of an actively mode-locked laser (which results from the timing jitter) also grows as n_h^2. However, for passively mode-locked lasers, such as the Ti:Sapphire system used in our work, widely varying behaviors have been predicted according to the assumed details of the statistics of the timing jitter[11]. For our 82 MHz passively mode-locked system (similar results are obtained for our 800 MHz system), we find the central core is broadened linearly with harmonic by laser power supply noise with $\Delta\nu/\nu \sim 3\times10^{-8}$. We also find a noise skirt around this central carrier whose amplitude grows as n_h^2 relative to the central core.

We will show that the timing jitter variations responsible for these observations are periodic, introduced via a parametric process resulting from gain modualtion of the Ti:sapphire by the Argon pump. Because the noise source is due to a parametric process, modulation theory is a more natural description than statistical noise theory, giving particularly simple and physically intuitive results. Additionally, we will show that the most basic spectral differences that have been predicted between actively and passively mode-locked systems are dependent upon the nature of the statistics of the assumed timing jitter. Finally, we will show that our passively mode-locked system has the spectral characteristics most commonly associated with actively mode-locked systems and that the physics which underlies this result should generally apply to many other mode-locked laser systems.

II. EXPERIMENT

Figure **1** shows the basic elements of the system. A Spectra Physics 2060 Argon Ion laser is used to pump either an 82 MHz or an 800 MHz Ti:Sapphire mode-locked laser. The 82 MHz system is of the conventional design pioneered by Spence *et al.*[5], while the 800 MHz system is a modification[6] of a design of Ramaswamy-Paye *et al.*[7]. The pulse train from either femtosecond laser is focused onto a Photo-Conductive Switch (PCS)[12, 13]. The PCS is integrated with a biased microwave antenna which has been sputtered onto the surface of a wafer of Low Temperature Grown GaAs (LTG GaAs). LTG GaAs has response times of ~250 fs, giving it a potential bandwidth of ~ 2 THz. The antenna allows radiation from PCS to be coupled into free space with a sapphire hemisphere. Because the characteristic impedance of the antenna structure is ~ 100 ohms, frequencies less than 8 GHz may be directly fed to the Tektronix 2782 Spectrum Analyzer via a short length of high frequency coaxial cable. To couple radiation at higher frequencies into the spectrum analyzer, a microwave horn was placed in front of the sapphire hemisphere. Above 100 GHz the Femtosecond Demodulation source output was mixed in an InSb photo-detector with an ISTOK millimeter-wave synthesizer to down convert it into the spectrum analyzer s range.

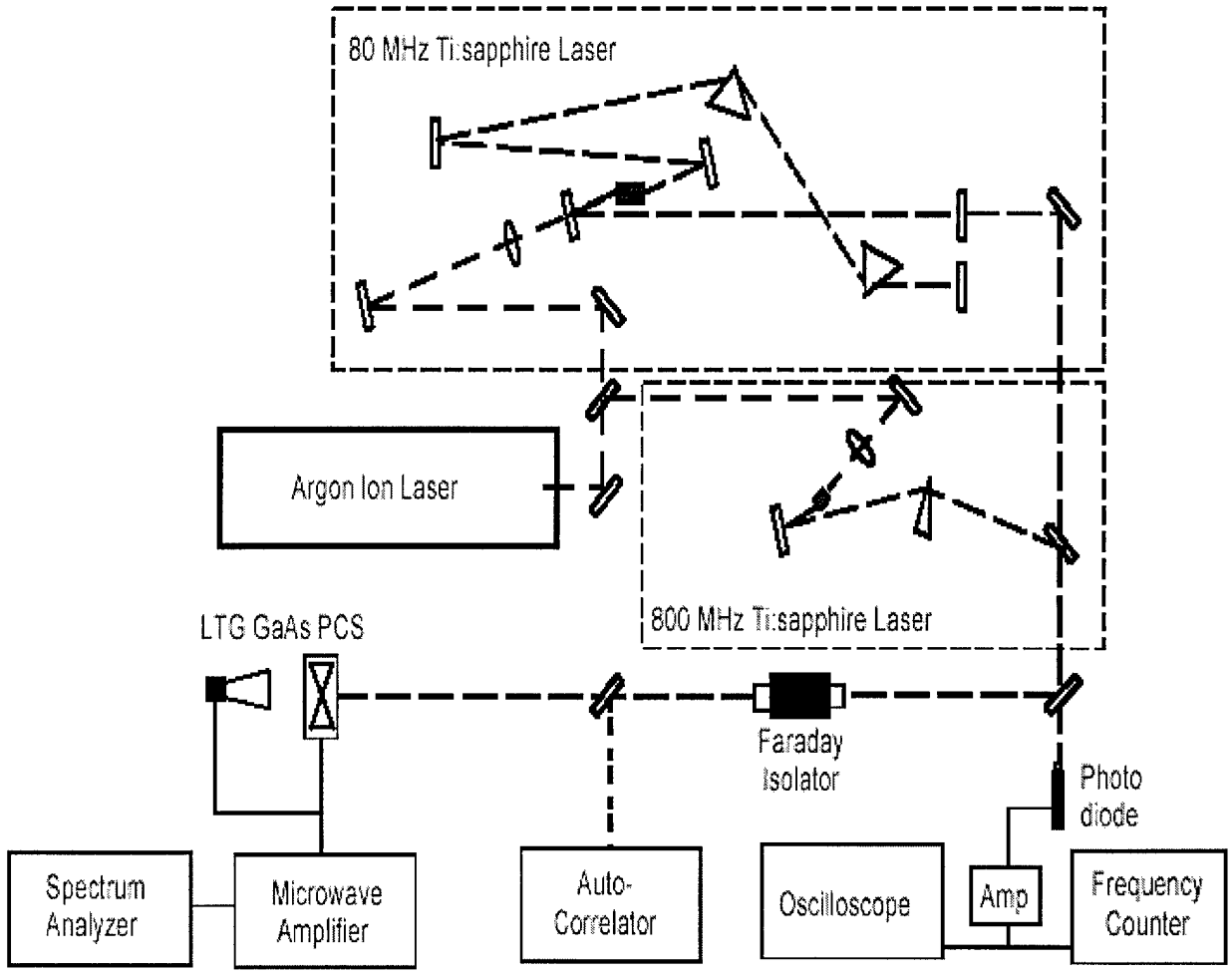

Figure 1. Elements of the Femtosecond Demodulation source and spectral analysis system.

III. EXPERIMENTAL RESULTS

In this section we will report spectral analysis measurements of the power spectrum of two different femtosecond demodulation sources. The first is driven by an 82 MHz passively mode-locked Ti:sapphire laser system and the second by an 800 MHz system. We will observe at low harmonic sidebands associated with power supply ripple that grow in amplitude as n^2. When these sidebands become comparable to the carrier in amplitude, higher order sidebands become significant and this core of modulation produced linewidth increases in width in proportion to harmonic. Additionally, we see a broad noise skirt whose amplitude also grows as n^2. We will also note a difference in the noise performance between the 82 and 800 MHz systems, which we will attribute to a change in the Ar^+ pump laser and a resulting change in its amplitude noise characteristics. Finally, in a later section we will show that the power spectra to very high harmonic of the Ti:Sapphire lasers can be accounted for in the context of modulation theory, with the modulation attributed to a combination of ~white and power supply induced ripple amplitude noise on the Ar^+ laser.

A. Power spectra of the 82 MHz laser

Figure **2(a)** shows the fundamental spectral component of the 82 MHz Ti:Sapphire mode-locked laser with a 30 Hz resolution bandwidth. 360 Hz sidebands (~ -45 dbc) are clearly observable and a broadening (~ -40 dbc) due to 180 Hz sidebands can also be seen. Figure **2(b)** shows the 20th harmonic. Again, the 360 Hz sidebands (~ - 20 dbc) are clearly observable, as are the 180 Hz sidebands and, at this harmonic, the noise pedestal. The dotted lines result from calculations that are discussed in a later section.

If a broader bandwidth is used, the individual sidebands associated with the 360 Hz ripple are not observed, but they contribute to the central line shape and width as is illustrated in Fig. **2(c-h)**. At the higher harmonics the broadening of the central core by the 360 Hz sidebands exceeds the resolution bandwidth of the spectrum analyzer. Consequently, the amplitude of the experimental spectrum is offset (based on a measurement of its width) so as to preserve the calibration of the power scale relative to an ideal delta function carrier. In Fig. **2(h)** the excess noise on either side of the central core is believed to be due to the lock loops in the KVARTZ synthesizer that was used as the local oscillator for this measurement.

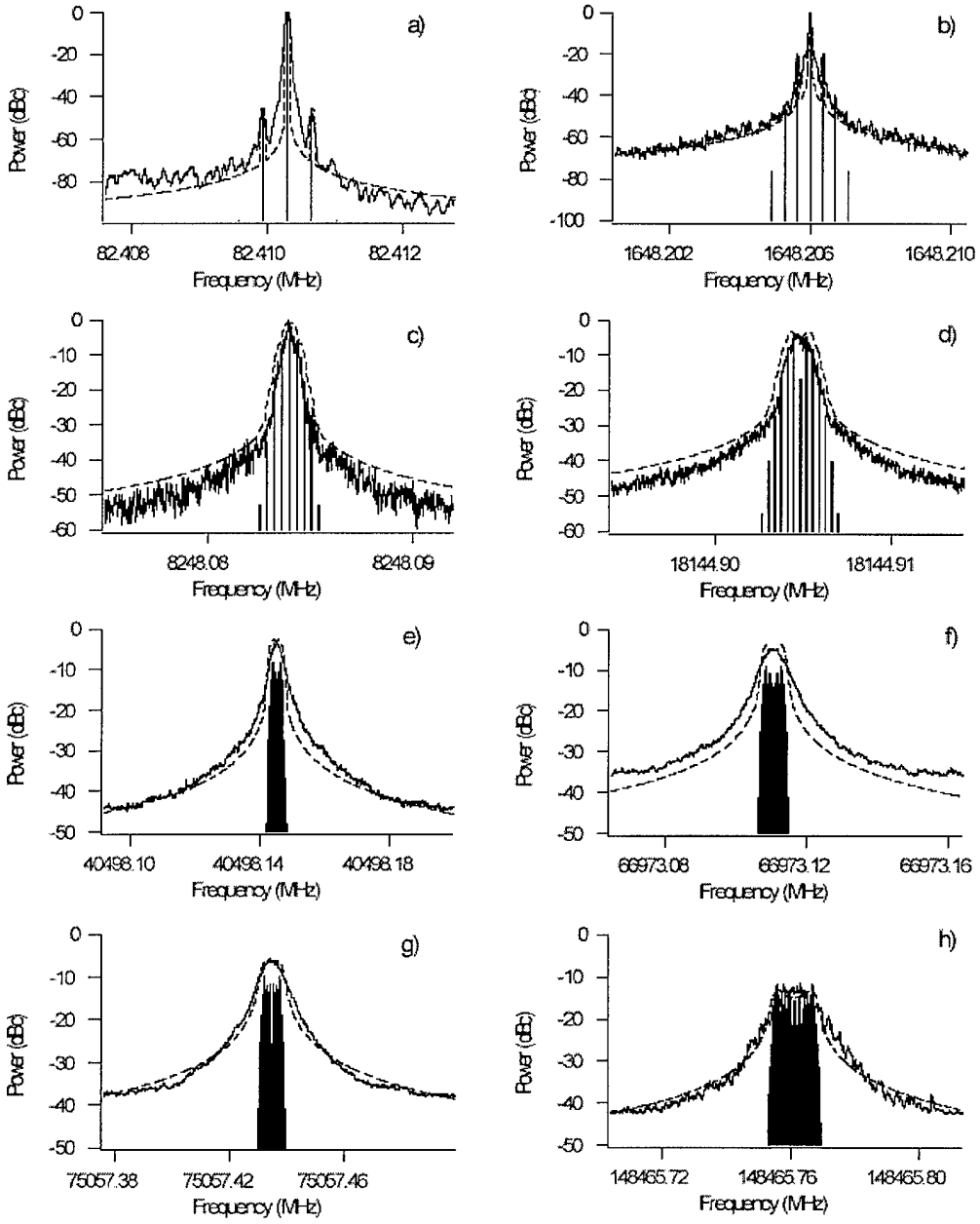

Figure 2. (a - b) Fundamental (82 MHz) and n = 20 spectral components observed with a resolution bandwidth (RBW) of 30 Hz. Visible are well resolved 360 Hz sidebands as well as smaller sidebands at 180 Hz. Both result from the power supply ripple on the Ar^+ laser. (c - h) The n = 100 (RBW = 300 Hz), 220 (RBW = 300 Hz), 494 (RBW = 1 kHz), 812 (RBW = 1 kHz), 910 (RBW = 1 kHz), and 1800 (RBW = 300 Hz) spectral components, respectively. The 360 Hz side-bands are not resolvable, but at these high harmonics multiple side-bands of the 360 Hz ripple make significant contributions to the width of the central core.

For all harmonics a broader pedestal, which is not resolvable into individual components, is also observable. The solid line is calculated from modulation theory with a modulation index of m_f = 3.5 Hz for the 360 Hz ripple and m_f = 0.035 $Hz^{1/2}$ for the ~white noise.

From a comparison of these measurements, we observe a central core which is dominated by harmonics of ripple frequencies (primarily 360 Hz) and that the amplitudes of these components grow as n_h^2 until they approach the amplitude of the carrier. As this occurs, new components at multiples of the fundamental ripple frequencies arise, giving an overall width to the central core, which grows linearly with the harmonic as shown in Fig. **3.** We also observe a pedestal which grows relative to the total carrier power as n_h^2 and which drops with frequency off-set from the carrier ($\Delta\nu_c$) slightly faster than $1/\Delta\nu_c^2$.

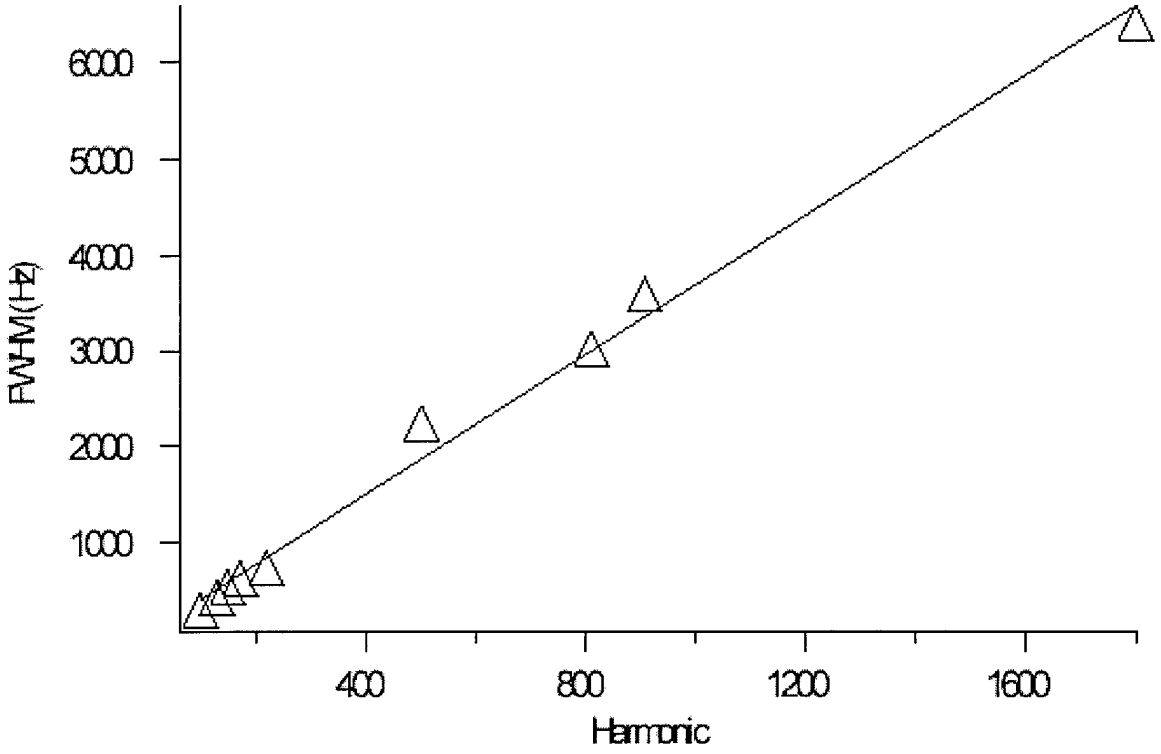

Figure 3. The FWHM line width as a function of harmonic number.

B. Power spectra of the 800 MHz Laser

Unfortunately, the Ar^+ pump laser used in the initial stages of this work failed rather early in its lifetime and its replacement had significantly different, and in general, worse noise characteristics. A further complication is that the Ar^+ pump replacement occurred as the 82 MHz Ti:Sapphire laser was replaced by the 800 MHz Ti:sapphire system. Figure **4** shows the fundamental spectral component of the 800 MHz Ti:Sapphire laser. We again see discreet features (especially at 360 Hz), but the overall noise of the system is such that it is more difficult to trace them in detail. We also observe a continuum pedestal which grows at a fixed off-set from the carrier ($\Delta\nu_c$) slightly faster than $1/\Delta\nu_c^2$.

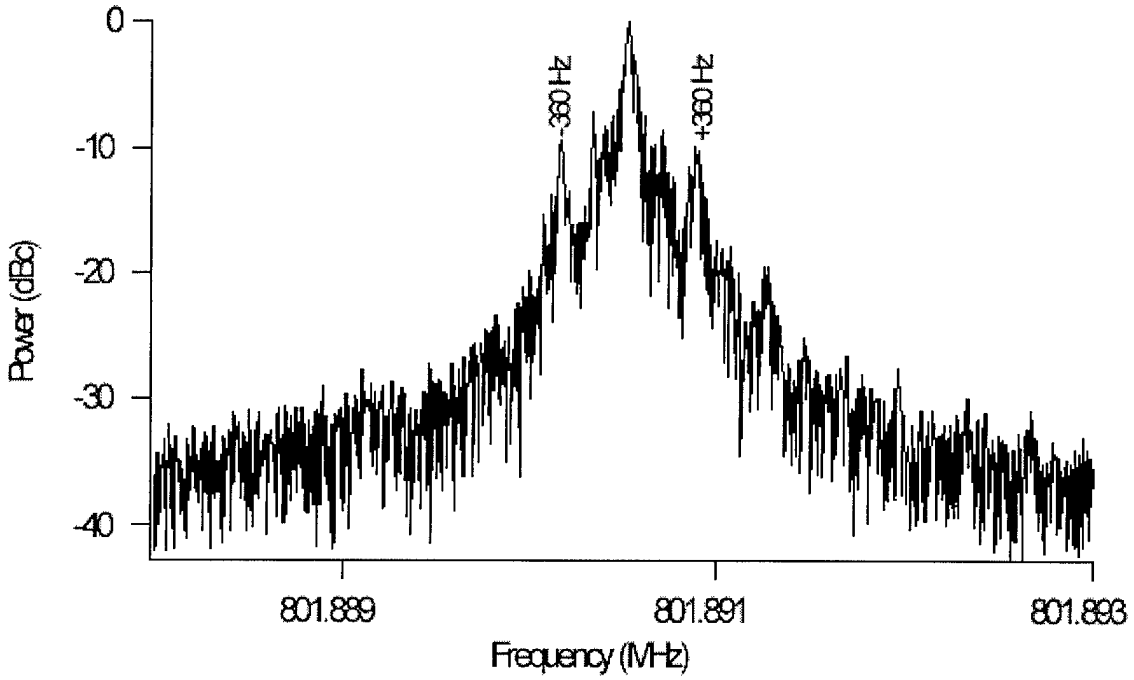

Figure 4. The fundamental spectral component of the 800 MHz mode locked Ti:Sapphire laser showing the 360 Hz sidebands and much more noise than observed with the 82 MHz laser.

C. Amplitude Noise on the Ar^+ Pump Lasers

Inspection of the data for the 82 MHz system pumped by the original Ar^+ laser clearly shows the effects of 360 Hz, and a lesser amount of 180 Hz and perhaps other periodic modulations over a wide range of harmonics. Because of the change in drive laser before we recorded the 800 MHz data, a much more complex combination of power supply induced modulations occurred in these observations. Inspection of the data for the 800 MHz system shows the modulation sidebands are more difficult to observe in the spectral analysis data, largely because of the larger continuum noise in the second pump laser, but also because of a variety of other variable low frequency noise sources. For instance, Figure **5** of the second harmonic of the 800 MHz laser clearly shows 30 Hz sidebands which broaden not only the central core, but the 360 Hz sidebands as well.

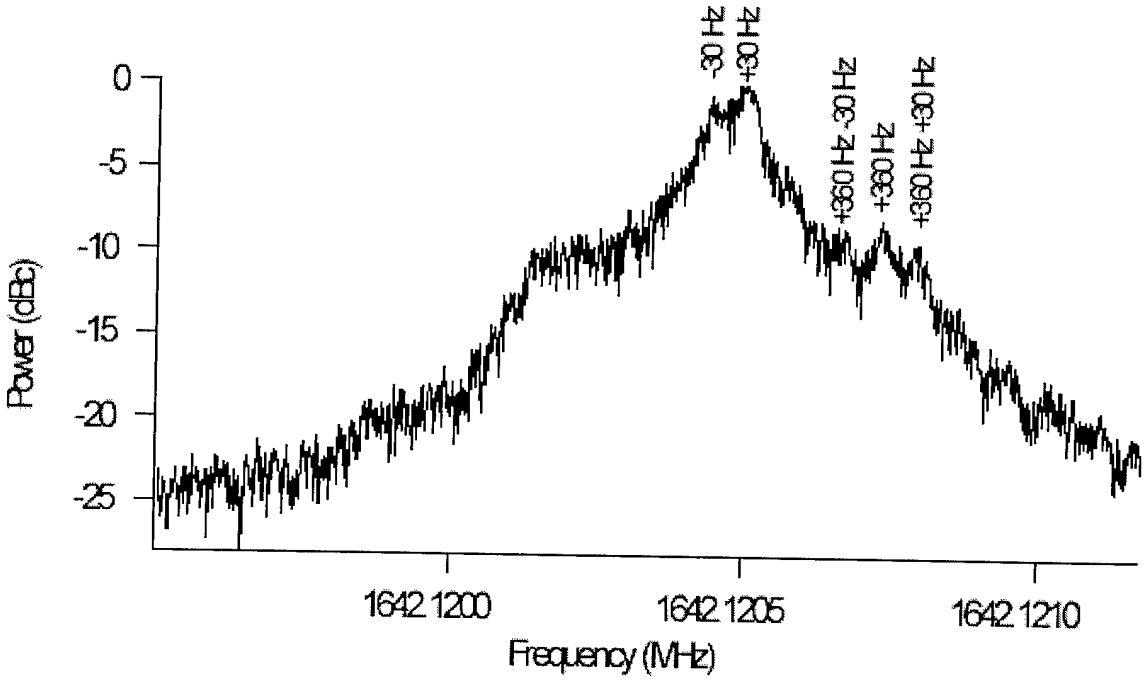

Figure 5. The second harmonic (n = 2) of the 800 MHz laser measured with a 30 Hz resolution bandwidth and showing broad 30 Hz sidebands of modulation index sufficient to broaden the central core and the 360 Hz sidebands.

If we make a simple temporal comparison between the Argon and Ti:Saphire amplitude noise we find the two are identical as shown in Figure 6.

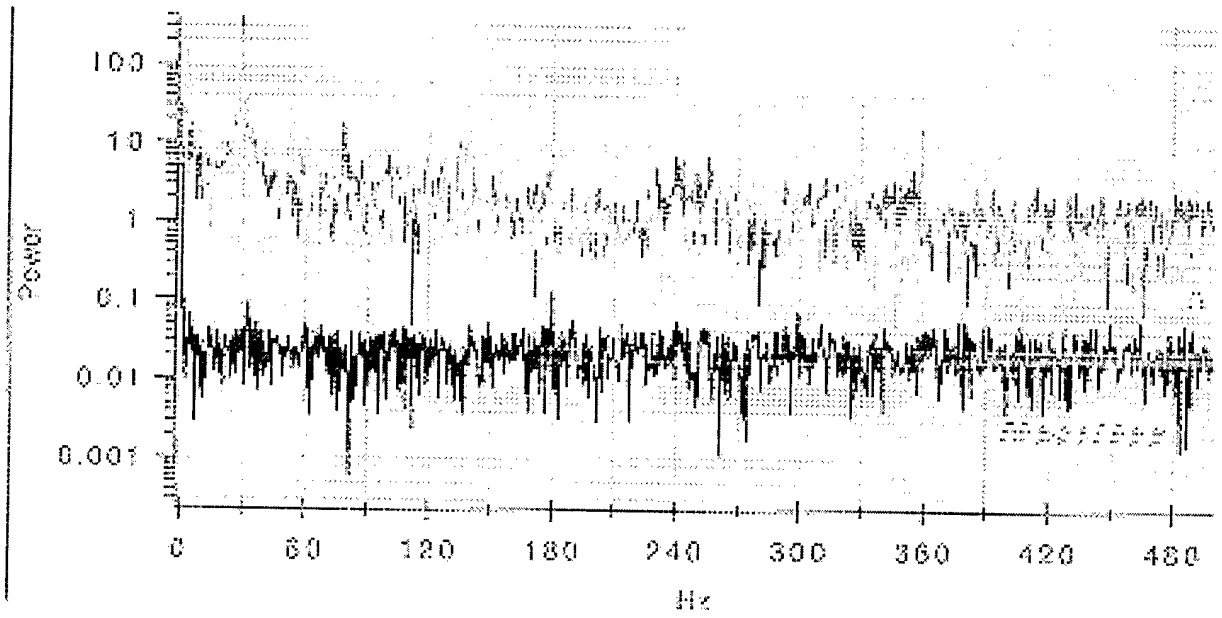

Figure 6: The top two traces are video detection of the Argon and the Ti:Saphire laser power outputs. The bottom trace is the noise flow of the detection system.

Because one of the goals is to develop a detailed understanding which relates the noise characteristics of the pump lasers, the timing jitter of the mode-locked lasers, and ultimately the spectral purity of our sources, we have developed an alternative to supplement the frequency domain spectral analysis comparison for this low frequency noise.

The time-domain frequency modulation waveform can be directly observed by use of the spectrum analyzer as an FM discriminator. With the spectrum analyzer scan turned off, the resolution bandwidth ν_R was set to be ~5 times *broader* than the modulation deviation of the mode-lock frequency and the post detection bandwidth of the spectrum analyzer ν_{PD} was chosen to be larger than the modulation frequency. By setting the inflection point of the spectrum analyzer response at the central mode-lock frequency, the FM modulation is translated by the discriminator action of this arrangement into an AM signal, which is then displayed as the output of the spectrum analyzer. In this arrangement the output is a pure function of time, rather than the complex mix of time and frequency which results for noise whose period is comparable to the scan time. Figure 7 shows a comparison of the AM directly measured on the Ar^+ pump laser and the output of the unscanned spectrum analyzer. The later is a direct observation of the timing jitter caused by the modulation. The modest differences between the two traces are due to modestly different bandwidths in the two systems and the variation in time of some of the low frequency noise.

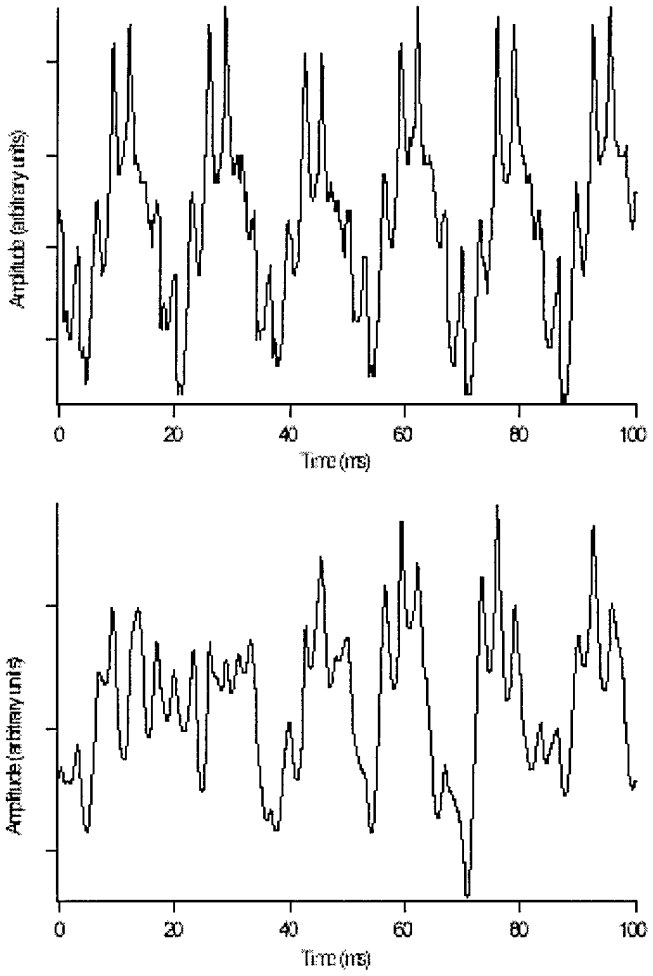

Figure 7. The AM on the Ar^+ pump laser (upper trace) and the frequency modulation waveform of the power spectrum of the Ti:Sapphire laser obtained by use of a spectrum analyzer as a frequency discriminator (lower trace).

Clearly observable in Figure 7 are peaks separated by 0.017 s, which are related to the 60 Hz power supply. The next most prominent features are at 360 Hz, a frequency related to ripple on 3-phase power supplies. Thus, the mode-lock frequency of the Ti:Sapphire laser has been linearly frequency modulated by the amplitude noise on the Ar^+ pump laser over the range of the ripple modulation (~10 - 500 Hz).

The spectral components of this noise can also be observed in the Fourier transform of the amplitude noise of **Fig. 7**, which is shown in **Fig. 8.** Here the power supply 60 Hz related noise can be observed, along with additional noise below 100 Hz. In addition to these narrow band contributions to the noise, a continuum of ~white noise extends to >100 kHz on the Ar^+ lasers. For example, between 100 Hz and 10 kHz a decrease of ~3 db has been observed[14]. Below we will show quantitatively that this continuum accounts for the noise skirts in Fig **2**.

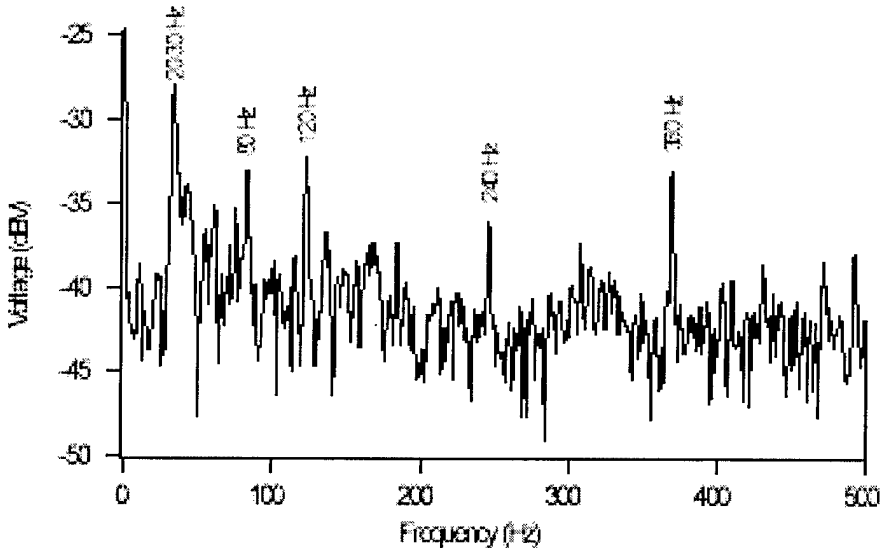

Figure 8. The Fourier transform of the AM waveform from Fig. 6.

IV. THEORY

The origins and magnitudes of pulse-to-pulse timing fluctuations and overall laser stability in mode-locked lasers have been topics of interest for some time. Initially, interest focused primarily on picosecond dye laser systems and was described in the seminal paper by von der Linde[9]. However, with the discovery and development of the Kerr induced, mode-locked, femtosecond Ti:Sapphire laser, much of this interest has been focused on these lasers and the study of noise phenomena on ever shrinking time-scales[5, 10]. Typically, noise models are developed in the time domain and use a Fourier transform to calculate a power spectrum[9-11, 15-17]. Conversely, from an observed power spectrum, the pulse-to-pulse variation, or jitter, may be calculated. Harvey et al. provide a concise description of this process[18].

In this section we will outline the development of the theory which relates timing jitter in short pulse lasers to spectral analysis. We will pay careful attention to retaining in the theory those elements necessary to account for the physical origins of noise. In particular, we will consider noise which is periodic and show in cases where periodic noise is important that passively mode-locked systems take on the characteristics ordinarily associated with actively mode-locked systems.

A. The Basic Relations

We will begin by developing the basic relations in the notation of Yariv[11, 16], but without the assumption that the noise which leads to width in the power spectrum is random. This will become important because it leads to significantly different predictions in technologically important cases. Because it has been shown that amplitude and shape fluctuations play similar roles in the power spectrum and that their roles becomes relatively less important at high harmonic, we will limit ourselves to consideration of the effects of timing jitter in a train of otherwise identical pulses.

In this context the timing variations in a train of n pulses can be described by

$$T_n = nT + \delta T_n \tag{1}$$

where T is the average time between pulses, T is the time of the n^{th} pulse, and δT is the variation of the n^{th} pulse around nT, where the δT may *either* be random or periodic. The intensity of a train of $2N + 1$ pulses can be described in the time domain as

$$I_{\Delta t}(t) = \sum_{n=-N}^{N} f_n(t - T_n) \tag{2}$$

where f_n is the n^{th} pulse intensity envelope in the train and Δt is the length of the pulse train.
Equivalently, in the frequency domain this train of pulses can be described by

$$P_I(\omega) = \frac{\lim}{\Delta t \to \infty} \left\langle I_{\Delta t}(\omega) I^*_{\Delta t}(\omega) \right\rangle \tag{3}$$

with

$$I_{\Delta t}(\omega) = \int_{-\Delta t/2}^{\Delta t/2} I_{\Delta t}(t) e^{i\omega t} dt \tag{4}$$

From this

$$I_{\Delta t}(\omega) = \sum_{n=-N}^{N} F_n(\omega) e^{i\omega T_n} \tag{5}$$

where

$$\mathrm{F_n}(\omega) = \int_{-\infty}^{\infty} f_n(t) e^{i\omega t} dt \tag{6}$$

The power spectrum of the pulse train is then

$$P_I(\omega) = \lim_{N\to\infty} \frac{1}{2N+1} \sum_{n,m=-N}^{N} e^{i\omega(T_n - T_m)} \left\langle F_n(\omega) F_m^*(\omega) \right\rangle \tag{7}$$

More explicitly, in terms of the timing jitter dTn

$$P_I(\omega) = \frac{\lim}{N \to \infty} \frac{1}{2N+1} \sum_{n,m=-N}^{N} e^{i\omega T(n-m)} \left\langle F_n(\omega) F_m^*(\omega) e^{i\omega(\delta T_n - \delta T_m)} \right\rangle \tag{8}$$

B. The Specific Cases

A number of sources of noise in mode locked lasers have been identified. These include gain, cavity length, refractive index, and spontaneous-emission fluctuations[16]. We will first review earlier work and then show the importance of choosing a natural description for the noise fluctuations that dominate many real laser systems.

Active mode lock:

Von der Linde has discussed the relation between fluctuations in the pulse trains of mode-locked lasers and their power spectra as observed by photodiodes and radio frequency (rf) spectral analysis techniques[9]. Because the laser system he studied was actively mode-locked, the timing fluctuations δT were relative to a continuously updated time standard. In such a system the long term spectral purity grows without bound, and in the frequency domain this results in a delta-function (limited only by the bandwidth associated with the observation time and the spectral purity of the active reference) central core. He also showed that the noise skirt associated with amplitude fluctuations is independent of harmonic n_h whereas the amplitude of the skirt characteristic of timing jitter grows as n_h^2.

Eliyahu, Salvatore, and Yariv have also discussed timing jitter and noise in actively mode-locked lasers[16]. With the assumption of stationary processes (from the active mode-lock) and a Gaussian probability distribution of the fluctuations in **Eq. 8** becomes

$$\left\langle e^{i\omega t(\delta T_n - \delta T_m)} \right\rangle = e^{-\omega^2 [G_T(0) - G_T(|n-m|)]} \tag{9}$$

where $G_T(k)$ is the timing-jitter autocorrelation function

$$G_T(k) = \langle \delta T_0 \delta T_k \rangle \tag{10}$$

and they too conclude that a delta function core results. More recently, Eliyahu, Salvatore, and Yariv[11] have explicitly considered the differences in the power spectrum of passively and actively mode-locked systems and also conclude for actively model-locked systems that the delta function core will be flanked by two pedestals: one which is independent of harmonic and due to amplitude fluctuations in the pulse train and the other whose amplitude increases with the square of the harmonic due to timing jitter fluctuations.

Random noise with passive mode lock:

In a passively mode-locked system with random timing jitter there is no absolute phase restoring influence and nonstationary statistics are appropriate[11]. This leads to a power spectrum in which the delta function of the actively mode-locked system is replaced by a central core of finite width. In the limit that the correlation time of the noise τ is less than the pulse repetition time T, a Lorentzian whose width increases with the square of the harmonic, but whose amplitude decreases with the square results. In the limit that the correlation time is long in comparison to T, a Gaussian whose width is proportional to harmonic number results. Eliyahu *et al.* have demonstrated experimentally the latter limit for the first 6 harmonics of the 608.5 MHz mode-lock frequency of a passively mode-locked semiconductor laser, with a normalized width ($\Delta\omega\, T/n$) of ~10^{-3}. This low spectral purity and the large timing jitter which causes it, result from the small mode volume of the semiconductor laser[17].

Periodic noise with passive mode lock:

In the passively mode-locked case it is possible to make other, non-random, assumptions about the noise which causes timing jitter and spectral width; specifically that the noise is periodic about a mean. Consider the case of noise which can be represented by a sum over terms of the form

$$\delta T_n = m_t \sin(2\pi \nu_m + \phi) \tag{11}$$

where m is the strength of the temporal fluctuation, i.e the magnitude of the temporal deviation. This replaces statistical noise fluctuation with a periodic temporal fluctuation. In their discussion of active mode locking with random fluctuations, Eliyahu *et al.* point out that because

$$\left\langle \left(\delta T_n - \delta T_m\right)^2 \right\rangle \approx 2\left[G_T(0) - G_T(|n-m|)\right] \tag{12}$$

(where the δT_n is measured relative to the external timing and $G_T(k) = \langle \delta T_0 \delta T_k \rangle$ is the autocorrelation of the timing-jitter fluctuations) is bounded, a central delta function results. More physically stated: with increasing observation time, the timing differences continue to shrink in comparison to the observation time because the differences are continually reset to an absolute timing point by the active mode-locking.

Likewise, in the case of periodic noise/modulation of **Eq. 11**, the timing error between the n^{th} and m^{th} pulse is also bounded, with the limit

$$\left\langle \left(\delta T_n - \delta T_m\right)^2 \right\rangle \approx m_t^{\,2} \tag{13}$$

and a central delta function also results, even in a passively mode-locked system.

C. Periodic Fluctuations

For lasers (such as Ar^+) with large mode volume many of the noise sources that lead to timing jitter and spectral width are, in fact, periodic and have their origins in microphonics, control loops, and imperfect power supplies. . these periodic noise sources modulate the optical path length of the laser resulting in a parametric mixing of the noise sources in the pump with the mode lock frequency. In these cases FM modulation theory provides detailed relationships between this noise and spectral observations which can be tested experimentally.

FM modulation theory:

Consider a model in which the fundamental mode-lock frequency of the laser is given by

$$\nu = \nu_0 + m_f \sin(2\pi\nu_m t + \phi) \qquad (14)$$

where $\nu_0 = 1/T$ is the fundamental mode lock frequency, ν_m the modulation frequency, and m_f the frequency amplitude of the modulation noise . For simplicity of notation, we will consider this example of a single noise frequency. It is well known[19] that frequency modulation leads to a spectrum containing sidebands separated from the fundamental mode-lock frequency ν_o by $\pm n\nu_m$, whose powers are given by

$$J_n^2(m_f/\nu_m) \qquad (15)$$

At the n_h^{th} harmonic of the mode lock frequency

$$\nu_h = n_h\left[\nu_0 + m_f \sin(2\pi\nu_m t + \phi)\right] \qquad (16)$$

and the corresponding sideband powers are

$$J_n^2(n_h m_f/\nu_m) \qquad (17)$$

An exact expression for the relation between the timing deviation m_t and frequency deviation m_f can be derived. If **Eq. 1** is expressed as

$$T_n = nT + m_t \sin(2\pi\nu_m t + \phi) \qquad (18)$$

then

$$\frac{1}{\nu_m} = T_{n+1} - T_n = T + m_t[\sin 2\pi\nu_m T_{n+1} - \sin 2\pi\nu_m T_n]$$

$$\frac{1}{\nu_m} = T + m_t T(2\pi\nu_m)\cos 2\pi\nu_m T_n \qquad (19)$$

$$\nu_m + \nu_0[1 - m_t(2\pi\nu_m)\cos 2\pi\nu_m t]$$

with $\nu_0 = \frac{1}{T}$, $t = T_n$, and $m_t = \frac{m_f}{2\pi\nu_m\nu_0}$.

This latter expression shows that the maximum *accumulated* timing error depends inversely on both the frequency of the modulation and the mode-lock frequency.

High modulation frequency limit :

In general, these sidebands have small amplitudes as long as ν_m (the modulation frequency) $> n_h m_f$, (the maximum frequency deviation at the harmonic). Because of this fundamental relation, spectral analyses of higher harmonics of the mode-lock frequency are more sensitive to high frequency noise. Additionally, spectral analysis techniques typically have high signal-to-noise and large dynamic range, which can be used to significantly increase the sensitivity of spectral analysis measurements to high frequency noise. Specifically, for $\nu_m >> n_h m_f$ only the first sideband is of significant amplitude and its power relative to the carrier power is given by

$$J_1^2(n_h m_f/\nu_m) = (1/4)(n_h m_f/\nu_m)^2 + \text{higher order terms} \qquad (20)$$

Thus, if 40 db of dynamic range is available, the modulation noise is unobservable only if $\nu_m < 100 n_h m_f$. This shows that not only is high harmonic spectral analysis an especially sensitive probe of high frequency noise, but also that such noise must be minimized for spectrally pure femtosecond demodulation THz sources. For example, Fig. **2** shows at the 82 MHz fundamental the 360 Hz sidebands are -45 dbc, but that by $n_h = 100$, they are of comparable magnitude.

If there are many noise modulation frequencies present for which $\nu_m >> n_h m_f$, each will produce a component of the noise spectrum at ν_m according to Eq. IV.D.7. Furthermore, the power amplitude of each component will grow with the square of the harmonic. If, additionally, this noise modulation is white , the overall noise spectrum will roll off as the square of the frequency offset from the carrier. Thus, periodic noise modulation also leads to the commonly observed and predicted noise skirt of constant shape whose amplitude grows with the square of the harmonic, for both actively [16] and passively [11] mode-locked lasers. Again, Fig. **2** shows this effect.

Low modulation frequency limit :

In contrast, for $\nu_m < n_h m_f$, many ($\sim n_h m_f/\nu_m$) modulation sidebands contain power approximately equal to that of the carrier frequency and as n_h grows, so does this number of significant sidebands and the spectral width of the source. Correspondingly, the amplitude of any of these components decreases as $\sim n_h$. This effect can be seen in Fig. **2**, above, which initially show the individually resolved components and at higher harmonic the linear growth of the width of the central core. A consequence of this bifurcation at $\nu_m \sim n_h m_f$ is that for the common case where the jitter/modulation noise exists over some range and where many harmonics are considered, the *shape* of the noise spectrum will change with harmonic.
Wewere able to fit the data to a Lorentzian shape and the signal to noise in the data did not allow the observation of a change in shape

.D. Summary

In summary, we conclude that while the non-stationary character of random noise in passively mode-locked lasers must lead to a broadening of the central core which grows with harmonic, periodic noise modulation is stationary and

systems dominated by periodic noise have spectral characteristics commonly ascribed to actively mode-locked systems. This result is most intuitive in its prediction of a central delta-function core for passively mode-locked systems dominated by periodic noise. However, modulation theory also predicts the phase noise skirt that grows as n_h^2 for high frequency noise components because of the expansion properties of the Bessel Function in **Eq. 20**.

V. THE PHYSICAL ORIGINS OF NOISE

There are a number of potential contributors to timing jitter in femtosecond mode-locked laser pulse trains and ultimately to the spectral purity of femtosecond demodulation sources. Most fundamental are quantum noise sources, which have been extensively discussed, especially theoretically[10, 20, 21]. However, as noted by Namiki, Yu, and Haus[17] these quantum noise sources are most significant in small mode volume semiconductor lasers and are in general difficult to observe in other lasers.

A convenient and widely used model for the physical origins of timing jitter is one which employs acoustic or vibrational changes in the cavity length[22]. While in dye laser based CPM systems jitter in the 100 — 400 Hz region has been attributed to bubbles in the dye[18] and cooling water induced jitter has been noted to cause a peak in the power spectrum in the 150 — 300 Hz region[23], there is little evidence to support mechanical vibrations as a major contributors. This is especially true at high frequencies where unreasonable accelerations would be required. Furthermore, mechanical vibrations should produce peaks in observed power spectra associated with particular mechanical modes. Such structures are generally not observed. Additionally, after noting that cavity length changes as small as 0.01μm at 100 Hz could cause a 5 ps timing jitter, Harvey et al. made a number of attempts at vibrational isolation and concluded that all attempts to reduce the noise spectrum via vibration isolation were at best inconclusive[18].

On the other hand, the Ar^+ pump lasers commonly used have a variety of noise sources which range from power supply and control loop electronics to noise associated with the laser discharge plasmas themselves. The most obvious of these can be associated with power supply ripple and are evidenced by pronounce peaks that can be observed in a number of published power spectra [9, 14, 22, 23].

Additionally, it has been noted the relatively long lifetime (3.2 μs) of the Ti:sapphire gain medium limits pump laser induced amplitude noise to a few hundred kHz[23], and that as a result Ti:sapphire amplitude noise at high frequency is very small.

Here we will provide a specific physical model that, in combination with the modulation theory discussed above, accounts for both the complex behavior at high harmonic of the modulation side-bands and also the behavior and magnitude of the observed noise skirts which grow as n_h^2.

In this model the amplitude noise (both the ~white and power supply induced ripple) of the Ar^+ pump laser modulates the gain of the Ti:sapphire laser and. This creates an effective change in optical path length within the Ti:sapphire gain medium transforming the amplitude noise of the pump laser into timing jitter/frequency modulation.. In the context of Eq. 14 abovee

$$m_f = \Delta P_{\text{pump}} D_{\text{FM/AM}} \tag{21}$$

where ΔP_{pump} is the power fluctuation on the Ar^+ laser and $D_{FM/AM}$ has the units of Hz/Watt and is determined by the physics that transforms the amplitude variation of the pump into the frequency modulation of the Ti:sapphire laser.

In order to evaluate physical processes, it is necessary to choose a mode geometry within the Ti:sapphire gain medium because many of the important parameters are intensity and geometry dependent. Unfortunately, this is difficult to with any certainty because of the well known nonlinear effects which lead to self-focusing, beam breakup, etc in Kerr media[24-27]. For simplicity in our calculations which are intended to establish the order of magnitude of the physical effects, we will assume a simple cylindrical mode of beam diameter 20μ [26].

The most obvious mechanisms are thermal and nonlinear. In the former the fluctuation in the power associated with

the pump laser cause fluctuations in the temperature of the crystal, thus changing the optical length of the crystal via the thermal coefficient of the index of refraction. In this case the speed required is that of the modulation frequency. For the ripple modulation this is primarily at 360 Hz, but for the ~white noise modulation it is much higher, extending in our observations to ~100 kHz. While the speed of the thermal process is marginally adequate, simple thermal calculations show that the effect is several orders of magnitude too small to account for the observed modulation.

For modulation associated with the optical non-linearity, it is the circulating peak power of the Ti:sapphire laser that is important. Clearly, optical non-linear processes are fast enough to produce the required modulation, but the magnitude of the effect must be established. Consider a nonlinear gain medium of index n_0 and non-linear index n_2. For simplicity we assume that the fractional fluctuations in both the pump and circulating Ti:Sapphire power and intensity are the same

$$\frac{\Delta P_{\text{pump}}}{P_{\text{pump}}} = \frac{\Delta P_{\text{cavity}}}{P_{\text{cavity}}} = f \tag{22}$$

Then the fluctuation induced change of optical length per unit length is

$$\frac{d(\Delta L)}{dz} = n_2 \Delta I \tag{23}$$

where ΔI is the change of intensity of the laser field in the crystal. If the fractional change in the intensity is also $f = \Delta I/I$, then

$$\frac{d(\Delta L)}{dz} = f n_2 I \tag{24}$$

Integration over the length of the crystal gives

$$\Delta L = f n_2 I L_{\text{xtal}} \tag{25}$$

or

$$\frac{\Delta \nu_0}{\nu} = \frac{\Delta L}{L} = f n_2 I \frac{L_{\text{xtal}}}{L} \tag{26}$$

For our 82 MHz laser

$$
\begin{aligned}
&P_{\text{cavity}} \approx 10^{6} W \\
&\frac{L_{\text{xtal}}}{L} \approx 10^{-2} \\
&n_2 = 3 \times 10^{-20}\, m^2/W \\
&f \approx 0.01
\end{aligned}
\tag{27}
$$

or

$$
\frac{\Delta \nu_0}{\nu_0} \approx 10^{-8} \tag{28}
$$

This is about a factor of 3 smaller than our experimental results and well within the uncertainties of the experiment.

Although, it would be possible to attempt a more detailed analysis of the mode properties of our two lasers, this is beyond the scope of this paper. We will adopt the alternative of using the well resolved power supply modulation sidebands in the observed power spectrum of the Ti:sapphire laser to establish the modulator parameter $D_{FM/AM}$ which corresponds to our optical configurations. We will then use this coefficient as a fixed parameter for the rest of our calculations.

VI. ANALYSIS AND DISCUSSION

In this section we will first compare and contrast two rather different passively mode-locked femtosecond laser systems: a semiconductor laser and an Ar^+ laser pumped Ti:sapphire laser. We will then consider more generally the skirts which grow as n_h^2 in a number of passively mode-locked systems. Finally, we will provide a quantitative analysis, based on the theory discussed above, which accounts for both the ripple modulated central core of our laser as well as the n_h^2 noise skirts described in Section III.

A. Two Passively Mode-Locked Systems

Because of the wide variety of passively mode-locked systems and especially of the condition under which they have been investigated, we will initially focus on two rather different systems: The Ar^+ laser pumped Ti:sapphire which is the subject of this paper and the semiconductor laser used by Eliyahu *et al.* to illustrate the theory which they have developed for passively mode-locked systems.

Eliyahu *et al.* showed that for passive mode-locked lasers, with the assumption of a Gaussian jitter spectrum and in the limit of long correlation time ($\tau_t >> T$) that the resulting harmonics of the power spectrum should have a Gaussian shape and a width given by

$$
\Delta\omega = 2\omega\sqrt{\langle \Delta T^2 \rangle \ln 2}\ /\ T \tag{29}
$$

where ΔT is the timing jitter between neighboring pulses. Since in a correlation time τ_t a jitter of

$$
\Delta T_{\tau_t} \approx \frac{\tau_t}{T} \Delta T \tag{30}
$$

is accumulated, the average of each such uncorrelated measurement of the frequency will have a fluctuation of the order

$$\frac{\Delta\omega}{2\omega} \approx \frac{\sqrt{\langle \Delta T_{\tau_t}^2 \rangle}}{\tau_t} \approx \frac{\sqrt{\langle \Delta T^2 \rangle}}{T} \tag{31}$$

which to a small numerical factor is the same as the detailed theory of Eliyahu, *et al.* For the semiconductor laser studied $\frac{\sqrt{\langle \Delta T^2 \rangle}}{T} \approx 1.9 \times 10^{-4}$ and the width of the observed Gaussian lineshape was found to increase linearly with frequency for the first 6 harmonics of the 608.5 MHz mode-lock frequency.

Consider first the predominate 360 Hz modulation on the 82 MHz Ti:sapphire system. It is important to note that $\frac{\sqrt{\langle \Delta T^2 \rangle}}{T} \approx 3 \times 10^{-8}$, approximately four orders of magnitude smaller than in the example of the semiconductor laser. As pointed out above, for $nm > \nu$ periodic modulation also results in a linewidth proportional to frequency but because this modulation is so small in comparison to that of the diode laser, it is only observed in high harmonic studies as reported in this paper. For comparison with the theory of Eliyahu *et al.* this width can be expressed as

$$\frac{\Delta\nu}{\nu} = \frac{m_f}{\nu_0} = \frac{2\pi\nu_m m_t \nu_0}{\nu_0} \tag{32}$$

But

$$m_t = \Delta T \frac{\nu_0}{\nu_m} \tag{33}$$

and

$$\frac{\Delta\nu}{\nu} \approx \frac{\sqrt{\langle \Delta T^2 \rangle}}{T} \tag{34}$$

Thus, on the enormously different time scales of the two experiments both theoretical approaches provide the intuitively satisfying uncertainty principle result for the linewidth and also the details of the observed lineshapes.

B. The n^2 Skirts

Now we will consider the additional features of our results as well as other observations of passively mode-locked systems. More specifically, the noise skirts whose amplitudes grow with the square of the harmonic. We have seen that these are a natural consequence of the theory of actively mode-locked lasers as well as our modulation theory of passively mode-locked systems.

It is important to note that physically both theories allow the existence of a central delta function core not allowed by passive mode-lock theory based on random processes. As is the case for active systems which obey stationary statistics due to the external timing reference, passive systems with periodic motion also obey stationary statistics because the location of the pulses relative to the ideal pulse train can not random-walk away, but rather must oscillate about the ideal location of the pulses.

The observed power spectrum of our passively mode-locked Ti:sapphire laser does not correspond to that predicted for passively mode-locked systems: For a Gaussian probability distribution of timing jitter and short correlation time ($\tau << T$), a Lorentzian shape whose width grows as the square of the harmonic, or for long correlation time ($\tau >> T$), a Gaussian whose width grows linearly with harmonic number. In fact, once the technical noise associated with the power-supply ripple is removed, it closely resembles that predicted for an actively mode-locked system: a central core, with a skirt that grows as n_h^2.

C. A Quantitative Relation between the Power Spectrum of Femtosecond Demodulation Sources and the Amplitude Noise on Ar^+ Pump Lasers

We have shown that the general features of the power spectrum we have obtained for a femtosecond demodulation source driven by two different mode-locked laser systems can be accounted for by FM modulation theory. We have also developed a model that relates the modulation indices which characterize this theory to the amplitude noise associated with the Ar^+ laser. For clarity of presentation in this section, we will separate the noise on the Ar^+ laser into two parts: a 360 Hz modulation associated with the power supply of the laser and a white noise spectrum due at least in part to the laser discharge. While this noise model is clearly too simple, the day-to-day variation in the Ar^+ laser noise make the complexity of a more detailed characterization unattractive. Moreover, the results of this model are not only very good, but are physically satisfying as well.

As discussed in Section V, the unknown details of the nonlinear propagation of the laser modes through the gain crystal preclude an absolute calculation of the experimentally observed spectral purity with no adjustable parameters. Accordingly, we use the 360 Hz sidebands seen in Figs. **2,** along with the corresponding 1% amplitude variation on the 5 W of Ar^+ laser power used to drive the Ti:sapphire laser, to calculate the modulation factor $D_{FM/AM}$ of Eq. **24**. Subsequently, we use the calculated $D_{AM/AM}$ to predict the observed noise skirts.

Inspection of the figures shows that the modulation index of $m = 3.5$ Hz reproduces the observed spectra over a very wide range of harmonics. Combining this with $\Delta P = 0.030\ W$ for the pump laser yields

$$D_{FM/AM} = 70\ Hz/W. \tag{35}$$

For white noise

$$m_f = m_f\ (BW)^{1/2} \tag{36}$$

where m_f is the modulation index associated with the noise in 1 Hz of bandwidth.

With the observation that the white noise in a 10 kHz bandwidth also is ~1% of the Ar^+ laser power

$$m_f = 0.035\ Hz^{1/2} \tag{37}$$

The solid lines in Fig. **2** are then calculated from these two indices. Inspection of the figures shows very satisfactory agreement. The resolved 360 Hz components agree very well over a range of harmonics. At the higher harmonics, the widths and shapes of the central core are also in good agreement, with the small differences in detail attributable to the use of a simple rectangular lineshape rather than a convolution of the spectrum analyzer response. The lowest harmonics were recorded with 30 Hz resolution bandwidth and show evidence of additional 180 Hz modulation, an effect that could easily be incorporated in the model.

While the agreement for the noise skirts is in some sense remarkable for a model with no adjustable parameters and a drive laser system with day-to-day variation in its noise characteristics, it is possible to note systematic deviations. These are mostly associated with the assumption of white laser noise. At low frequency, near the carrier, the experimental noise exceeds that of the model. Additionally, at high frequency, the experimentally observed noise falls somewhat more slowly than that calculated from the white model. While the latter could be modeled with a small roll off in the white spectrum, the former was often time dependent.

VII. SUMMARY AND CONCLUSIONS

In this paper we have reported direct measurements of the spectral purity of a femtosecond demodulation THz source at high harmonic by use of spectral analysis techniques. We have also developed a theoretical framework for the analysis of our results based on a frequency modulation model of the timing jitter in our passively mode-locked

Ti:sapphire laser driver and have considered the relations between the parameters in this model and the underlying physics of the system.

For our femtosecond demodulation systems we have found:

1. The central core of the observed spectrum for the 82 MHz system can be model to high accuracy over a large harmonic range with FM modulation theory. Furthermore, the physical origin of this noise is primarily power supply ripple on the Ar^+ laser. Due to increased and complex low frequency noise in the Ar^+ laser used to pump our 800 MHz system, the modeling of the ripple noise on this system was not carried out over as wide an harmonic range or in as much detail. However, all of our observations could be modeled with the same theory.

2. In the limit $\nu > n m$ a pair of sidebands, which grow as n^2, were observed around the central carrier at the ripple frequency(δ). In the high harmonic limit, the power supply modulation is large enough so that $\nu << n m$. In this limit this central modulation core grows linearly with harmonic and a source Q of 3×10^{11} results for the 82 MHz system. This Q is simply the fractional frequency deviation of the mode-lock frequency induced by the amplitude noise on the Ar^+ pump laser. Because this noise source is related to power supply shortcomings, it is not fundamental and can be reduced if higher spectral purity is required.

3. In addition we observe for both the 82 MHz and 800 MHz systems broad noise skirts whose amplitudes relative to the carrier power grow as n^2 and decrease as $\sim 1/\Delta\nu^2$ where $\Delta\nu$ is the off set from the carrier frequency. The same mathematical and physical model that is used to relate the spectrum of the central core to the ripple on the Ar^+ laser is used to related these skirts to the ~ white amplitude noise of the Ar^+ laser, without the introduction of any adjustable parameters.

4. The behavior of the noise skirts observed in the spectra of our passively mode-locked systems is more characteristic of that which has been predicted for actively mode-locked systems than for passively mode-locked systems. This is a direct result of periodic noise not accumulating phase error as do many kinds of random noise.

Thus, we conclude the technical noise of our lasers is predominately periodic. As a result the spectral purity of our femtosecond demodulation sources is very high, currently exceeding by ~two orders of magnitude that required for high resolution Doppler limited spectroscopy. Furthermore, this spectral purity is not fundamentally limited and either an improvement in the power supply of the Ar^+ pump laser or its replacement would further improve the spectral purity of the system.

VIII. ACKNOWLEDGEMENTS

I would like to thank the participation of Kimberly Ann Juvan, Frank DeLucia, J. Swartz, T.M. Goyette, J.O. Everitt and J. R. Demers.

REFERENCES:

IX. References

[1] T. M. Goyette, W. Guo, F. C. De Lucia, J. Swartz, H. O. Everitt, B. D. Guenther, and E. R. Brown, Femtosectond Demodulation Source for High Resolution Submillimeter Spectroscopy, *Appl. Phys. Lett.*, vol. 67, pp. 3810-3812, 1995.

[2] F. C. De Lucia, B. D. Guenther, and T. Anderson, Microwave Generation from Picosecond Demodulation Sources, *Appl. Phys. Lett.*, vol. 47, pp. 894-896, 1985.

[3] D. H. Auston, K. P. Cheung, and P. R. Smith, Picosecond Photoconducting Hertzian Dipoles, *Appl. Phys. Lett.*, vol. 45, pp. 284-286, 1984.

[4] N. Katzenellenbogen and D. Grischkowsky, Ef ficient generation of 380 fs pulses of THz radiation by ultrafast laser pulse excitation of a biased metal semiconductor interface, *Appl. Phys. Lett.*, vol. 58, pp. 222-224, 1991.

[5] D. E. Spence, P. N. Kean, and W. Sibbett, 60-fsec pulse generation from a self-mode-locked Ti:sapphire laser, *Opt. Lett.*, vol. 16, pp. 42-44, 1991.

[6] J. R. Demers and F. C. De Lucia, Modulating and Scanning the Mode-lock Frequency of a 800 MHz Femtosecond Ti:sapphire Laser, *Opt. Lett.*, vol. 24, pp. 250-252, 1999.

[7] M. Ramaswamy-Paye and J. G. Fujimoto, Compact dispersion-compensating geometry for Kerr -lens mode-locked femtosecond lasers, *Opt. Lett.*, vol. 19, pp. 1756-1758, 1994.

[8] B. E. Bouma and J. G. Fujimoto, Compact Kerr -lens mode-locked resonators, *Opt. Lett.*, vol. 21, pp. 134-136, 1996.

[9] D. von der Linde, Characterization of the Noise in Continuously Operating Mode-Locked Lasers, *Appl. Phys. B*, vol. 39, pp. 201-217, 1986.

[10] H. A. Haus and A. Mecozzi, Noise of Mode-Locked Lasers, *IEEE J. Quant. Electron.*, vol. 29, pp. 983-996, 1993.

[11] D. Eliyahu, R. A. Salvatore, and A. Yariv, Ef fect of noise on the power spectrum of passively mode-locked lasers, *J. Opt. Soc. B*, vol. 14, pp. 167-174, 1997.

[12] E. R. Brown, K. A. McIntosh, F. W. Smith, K. B. Nichols, M. J. Manfra, and C. L. Dennis, Milliwatt output and superquadratic bias dependence in a low-temperature-grown GaAs photomixer, *Appl. Phys. Lett.*, vol. 64, pp. 3311-3313, 1994.

[13] E. R. Brown, K. A. McIntosh, K. B. Nichols, and C. L. Dennis, Photomixing up to 3.8 THz in low-temperature-grown GaAs, *Appl. Phys. Lett.*, vol. 66, pp. 285-287, 1995.

[14] A. Poppe, L. Xu, F. Krausz, and C. Spielmann, Noise Characterization of Sub-10-fs Ti:Sapphire Oscillators, *IEEE J. Selected Topics in Quantum Electron.*, vol. 4, pp. 179-184, 1998.

[15] L. P. Chen, Y. Wang, and J. M. Liu, Spectral Measurement of the Noise in Continuous-W ave Mode-Locked Laser Pulses, *IEEE. J. Quantum Electron.*, vol. 32, pp. 1817-1825, 1996.

[16] D. Eliyahu, R. A. Salvatore, and A. Yariv, Noise characterization of a pulse train generated by actively mode-locked lasers, *J. Opt. Soc. Am. B*, vol. 13, pp. 1619-1626, 1996.

[17] S. Namiki, C. X. Yu, and H. A. Haus, Observation of nearly quantum-limited timing jitter in an all-fiber ring laser, *J. Opt. Soc. Am. B*, vol. 13, pp. 2817-2823, 1996.

[18] G. T. Harvey, M. S. Heutmaker, P. R. Smith, M. C. Nuss, U. Keller, and J. A. Valdmanis, T iming Jitter and Pump-Induced Amplitude Modulation in the Colliding-Pulse Mode-Locked (CPM) Laser, *IEEE J. Quantum Electron.*, vol. 27, pp. 295-301, 1991.

[19] A. B. Bronwell and R. E. Beam, *Theory and Application of Microwaves*. New York: McGraw-Hill Book Co., 1947.

[20] D. v. d. Linde, Characterization of the Noise in Continuously Operating Mode-Locked Lasers, *Appl. Phys. B*, vol. 39, pp. 201-217, 1986.

[21] C. X. Yu, S. Namiki, and H. A. Haus, Noise of the Stretched Pulse Fiber Laser : Part I - Theory, *IEEE Journal of Quantum Electronics*, vol. 33, pp. 649-659, 1997.

[22] D. R. Walker, D. W. Crust, W. E. Sleat, and W. Sibbett, Reduction of Phase Noise in Passively Mode-Locked Lasers, *IEEE J. Quantum Electron.*, vol. 28, pp. 289-296, 1992.